European Radiology (2019) 29:689–698
https://doi.org/10.1007/s00330-018-5624-7

VASCULAR-INTERVENTIONAL

The role of wall shear stress in the parent artery as an independent variable in the formation status of anterior communicating artery aneurysms

Xin Zhang[1] · Zhi-Qiang Yao[1,2] · Tamrakar Karuna[3] · Xu-Ying He[1] · Xue-Min Wang[4] · Xi-Feng Li[1] · Wen-Chao Liu[1] · Ran Li[1] · Shen-Quan Guo[1] · Yun-Chang Chen[1] · Gan-Cheng Li[1] · Chuan-Zhi Duan[1]

Received: 10 April 2018 / Revised: 1 June 2018 / Accepted: 21 June 2018 / Published online: 17 July 2018

Abstract

Objectives The study aimed to determine which hemodynamic parameters independently characterize anterior communicating artery (AcomA) aneurysm formation and explore the threshold of wall shear stress (WSS) of the parent artery to better illustrate the correlation between the magnitude of WSS and AcomA aneurysm formation.

Methods Eighty-one patients with AcomA aneurysms and 118 patients without intracranial aneurysms (control population), as confirmed by digital subtraction angiography (DSA) from January 2014 to May 2017, were included in this cross-sectional study. Three-dimensional-DSA was performed to evaluate the morphologic characteristics of AcomA aneurysms. Local hemodynamic parameters were obtained using transcranial color-coded duplex (TCCD). Multivariate logistic regression and a two-piecewise linear regression model were used to determine which hemodynamic parameters are independent predictors of AcomA aneurysm formation and identify the threshold effect of WSS of the parent artery with respect to AcomA aneurysm formation.

Results Univariate analyses showed that the WSS ($p < 0.0001$), angle between the A1 and A2 segments of the anterior cerebral artery (ACA) ($p < 0.001$), hypertension (grade II) ($p = 0.007$), fasting blood glucose (FBG; > 6.0 mmol/L) ($p = 0.005$), and dominant A1 ($p < 0.001$) were the significant parameters. Multivariate analyses showed a significant association between WSS of the parent artery and AcomA aneurysm formation ($p = 0.0001$). WSS of the parent artery (7.8-12.3 dyne/cm^2) had a significant association between WSS and aneurysm formation (HR 2.0, 95% CI 1.3-2.8, $p < 0.001$).

Conclusions WSS ranging between 7.8 and 12.3 dyne/cm^2 independently characterizes AcomA aneurysm formation. With each additional unit of WSS, there was a one-fold increase in the risk of AcomA aneurysm formation.

Key Points

- *Multivariate analyses and a two-piecewise linear regression model were used to evaluate the risk factors for AcomA aneurysm formation and the threshold effect of WSS on AcomA aneurysm formation.*
- *WSS ranging between 7.8 and 12.3 dyne/cm^2 was shown to be a reliable hemodynamic parameter in the formation of AcomA aneurysms. The probability of AcomA aneurysm formation increased one-fold for each additional unit of WSS.*
- *An ultrasound-based TCCD technique is a simple and accessible noninvasive method for detecting WSS in vivo; thus, it can be applied as a screening tool for evaluating the probability of aneurysm formation in primary care facilities and community hospitals because of the relatively low resource intensity.*

Xin Zhang and Zhi-Qiang Yao contributed equally to this work.

✉ Chuan-Zhi Duan
doctor_duanzj@163.com

[1] National Key Clinical Specialty/Engineering Technology Research Center of Education Ministry of China, Guangdong Provincial Key Laboratory on Brain Function Repair and Regeneration, Neurosurgery Institute, Department of Neurosurgery, Zhujiang Hospital, Southern Medical University, 253# industry road, Guangzhou 510282, Guangdong, China

[2] Department of Interventional Neuroradiology, the First Affiliated Hospital of Zhengzhou University, Zhengzhou 450052, China

[3] Department of Neurosurgery, CMS-Teaching Hospital, Bharatpur, Chitwan 44200, Nepal

[4] Key Laboratory of Psychiatric Disorders of Guangdong Province, Department of Neurobiology, School of Basic Medical Science, Southern Medical University, Guangzhou 510000, China

Keywords Anterior communicating artery aneurysm · Hemodynamics · Risk

Abbreviations and acronyms

ACA	Anterior cerebral artery
AcomA	Anterior communicating artery aneurysm
CAD	Coronary artery disease
CFD	Computational fluid dynamics
CTA	Computed tomography angiography
CWT	Circumferential wall tension
DBP	Diastolic blood pressure
DSA	Digital subtraction angiography
FBG	Fasting blood glucose;
ID	Internal diameter
MRA	Magnetic resonance angiography
SBP	Systolic blood pressure
TCCD	Transcranial color-coded duplex
WSS	Wall shear stress

Introduction

The anterior communicating artery (AcomA) is recognized as the predilection site for intracranial aneurysms, accounting for > 25% of all intracranial aneurysm populations [1, 2]. The AcomA also carries higher risk of rupture than other locations in the anterior circulation. The complexity of the geometry in the AcomA determines the diversity in flow conditions, which makes AcomA aneurysms the most complex within the anterior circulation [3].

Despite the large number of animal experiments and clinical studies, the pathogenesis of intracranial aneurysm formation is still unclear. A growing number of studies based on numeral simulation of computational fluid dynamics (CFD) techniques have demonstrated that hemodynamics are essential to understanding AcomA aneurysm formation [4, 5]. Wall shear stress (WSS) is a flow-induced stress acting on the endothelial surface and can be described as the frictional force of viscous blood [3, 6]. WSS is recognized as a critical determinant of vessel diameter and is implicated in vascular remodeling [7]. In recent years, an increasing number of studies have demonstrated that WSS is closely related to determining aneurysm initiation, growth, and rupture [4, 5, 8–10]. Although WSS is widely reported in the process, there is no agreement on whether or not regions of low or high flow are most critical in promoting the events responsible for aneurysm formation. The growing number of such proposals has been controversial. Indeed, the accurate criterion for low or high levels of WSS related to AcomA aneurysm formation is unclear.

In this study, we identified which hemodynamic parameters independently characterized the formation of AcomA aneurysms using multivariate logistic regression and determined the WSS threshold in the parent artery using two-piecewise linear regression models to better illustrate the correlation between the magnitude of WSS and AcomA aneurysm formation. We also sought more simplified and convenient alternative techniques to detect WSS as a screening tool for evaluating the risk of aneurysm formation in primary care facilities and community hospitals in China and many developing countries because of the relatively low resource intensity.

Materials and methods

Study population

Approval for this study was obtained from the local Institutional Review Board of the participating centers. The study included consecutive patients who were diagnosed with single AcomA aneurysms, and participants without intracranial aneurysms served as the control population. All patients were admitted to the hospital with a suspected intracranial aneurysm detected by magnetic resonance angiography (MRA) or computed tomography angiography (CTA) examination and underwent digital subtraction angiography (DSA) after admission. The exclusion criteria were as per the study conducted by Kaspera et al [11].

Eighty-one consecutive patients with single, unruptured AcomA aneurysms and 118 participants without intracranial aneurysms were included in this cross-sectional study at Southern Medical University Zhujiang Hospital and the First Affiliated Hospital of Zhengzhou University from January 2014 to May 2017.

Evaluation of morphologic and hemodynamic characteristics (Fig. 1)

Three-dimensional-DSA was performed in all patients after admission. Specific geometrical patterns were reconstructed from 3D-DSA images to confirm the morphologic structure. Morphologic parameters, such as a dominant A1 and the angle between the A1 and A2 segments of the anterior cerebral artery (ACA), were defined and measured, as described in a previous study [12].

Transcranial color-coded duplex (TCCD) was performed with a Philips EPIQ5 ultrasound system (Philips; Washington, USA), which includes a 2.0-MHz real-time imaging transducer and a 2.0-MHz pulsed Doppler transducer. The maximum *in situ* Doppler energy output intensity was 89 mW/cm^2 spatial peak time average intensity ($I_{STPA.3}$). TCCD was performed by the same examiner. The ACA was imaged using a transtemporal window with the patient in the supine position [13]. The mean blood flow velocity (Vm) was

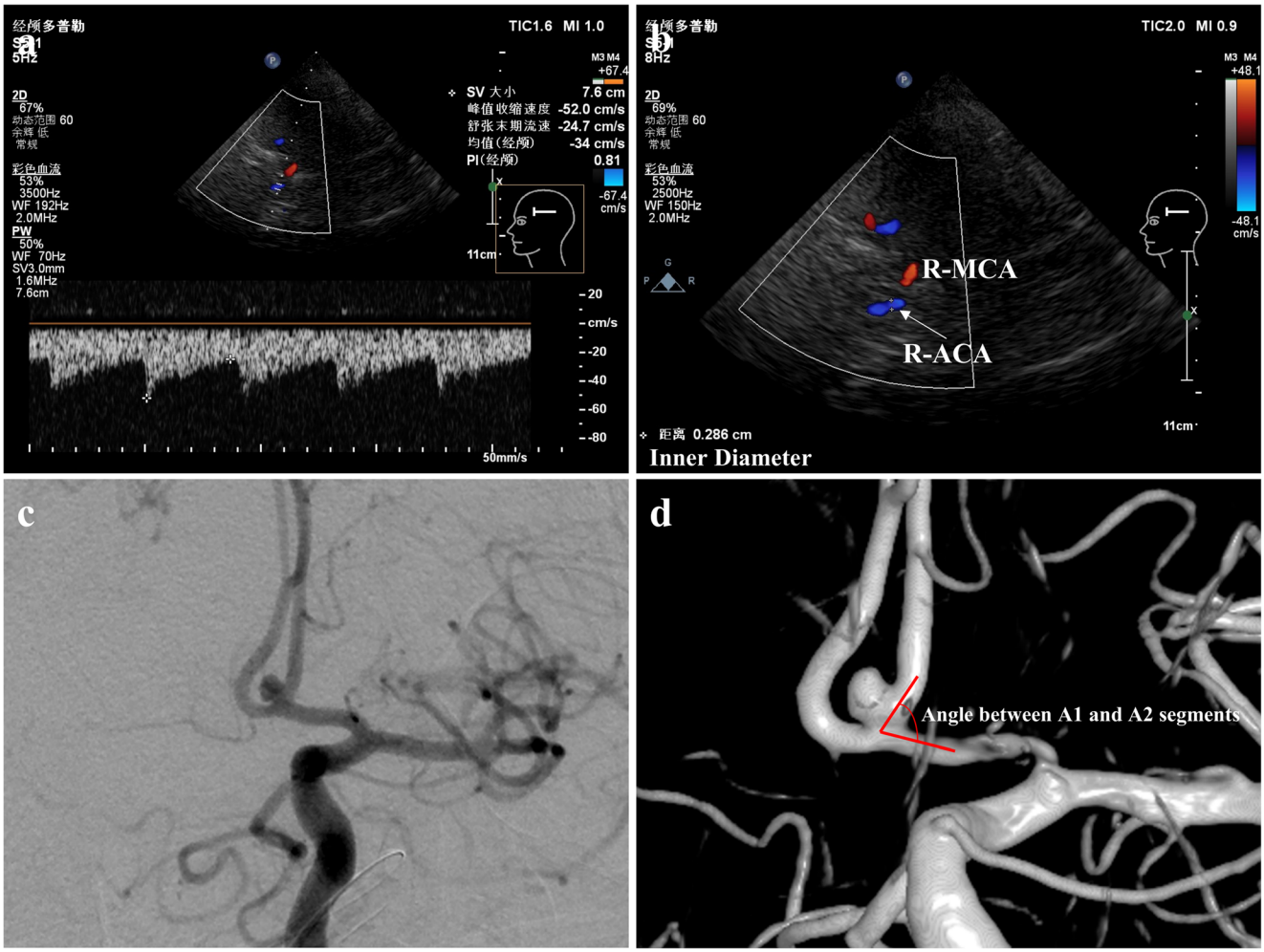

Fig. 1 An ultrasound-based TCCD technique and reconstructed 3D-DSA image showing the measurements in ACA. **a, b** Doppler measurements in right ACA (white arrow, blue blood flow signal). **c**, **d** 2D-DSA and reconstructed 3D-DSA images for measuring morphologic parameters of ACA aneurysm

measured for the bilateral distal end of each A1 segment of the ACA [14]. An ultrasound probe was placed as close as possible to the distal end of each A1 segment, and the lateral and paramedian frontal bone windows were used for accurate detection, according to the procedure described by Stolz et al [15]. Each TCCD examination was performed with the sample volume being placed within the color flow image of the examined artery.

In the case of aplasia of the A1 segment, these measurements were applied only to the dominant A1 segment. If the A1 segments were symmetric, the parameters were measured at the ipsilateral A1 in aneurysm cases and at the side with faster blood flow velocity in cases without aneurysms.

The internal diameter (ID) of the distal end of the ACA was measured between the leading edge of the echo produced by the intima-lumen interfaces of the near and far walls of the A1 segments at the R (ID_R) and T (ID_T) waves of the electrocardiogram, representing the minimum and maximum diameters, respectively [14]. Images of the interfaces between the lumen and intima were captured over five cardiac cycles and stored.

Blood viscosity (η) was measured in vitro at 37°C using a cone-plate viscometer and recorded at a shear rate of 200 s^{-1}.

Systolic blood pressure (SBP) and diastolic blood pressure (DBP) were measured on the right arm using a calibrated, fully automated device (Omron HEM-705-CP; Tokyo, Japan) after the participant had rested for at least 5 min on at least two occasions. According to the formula of Wiggers, the average of the second and third of three readings was computed. The mean blood pressure (MBP) was computed as DBP + one-third of the differential pressure.

Hemodynamic parameter calculations

The vessel wall is assumed to be rigid, with blood as a Newtonian fluid. Mean WSS is calculated by the Poiseuille law according to the following formulas [14]: $WSS_m = 4 \times \eta \times$

V_m/ID (dyne/cm^2), where V_m is expressed in centimeters per second and ID in centimeters and η in mPa·s.

Mean circumferential wall tension (CWT_m) is calculated by the Laplace law according to the following formula [16]: CWT = MBP × (ID/2) (dyne/cm^2), where MBPs are expressed in dynes/cm^2 and mean ID in diameters in cm.

Sometimes an accidental rise in the WSS of the parent artery can occur as part of normal daily blood pressure variance. If a significantly higher WSS was detected while the blood pressure was raised, we suggested repeating the measurement after the participant had rested for at least 5-10 min.

Note: CWT is tensile stress divided by wall thickness. CWT acts perpendicularly to the arterial wall and results from the dilating effect of blood pressure on the vessel [17].

Statistic analysis

Continuous variables were expressed as mean ± standard deviation (normal distribution) or median (quartile) (skewed distribution). Categorical variables were expressed in frequency or as a percentage. The *t* test (normal) or one-way ANOVA, Mann-Whitney (skewed distribution) or Kruskal-Wallis H test and chi-square tests (categorical variables) were used to determine any statistical difference between the means and proportions of the WSS groups. $p < 0.05$ (two-sided) was considered statistically significant. Multiple WSS models were used to evaluate the associations between exposure (WSS) and outcome (AcomA aneurysm formation). Both non-adjusted and multivariate adjusted models were used. A two-piecewise linear regression model was used to examine the threshold effect of the WSS on the AcomA aneurysm formation according to the smoothing plot. The threshold level of WSS at which the relationship between the AcomA aneurysm formation and WSS level began to change and became notable was determined using a recurrence method. The inflection point was moved along a pre-defined interval and detected the inflection point that gave the maximum model likelihood.

All analyses were performed with R (R Foundation for Statistical Computing, Vienna, Austria) and EmpowerStats (X&Y Solutions, Inc., Boston, MA, USA).

Results

Baseline characteristics of participants

The baseline characteristics of participants are shown in Table 1. The statistical results showed that there was a statistically significant difference in aneurysm morphology, coronary artery disease (CAD) and dominant A1 among the categorical variable (quartile) groups of WSS.

Univariate analysis for each parameter variable

The results of univariate analysis are shown in Table 2, demonstrating that the WSS ($p < 0.0001$), the angle between the A1 and A2 segments of ACA ($p < 0.001$), hypertension (grade II) ($p = 0.007$), fasting blood glucose (FBG; > 6.0 mmol/L) ($p = 0.005$), and dominant A1 ($p < 0.001$) were significant parameters.

Multivariate Analyses

We chose WSS for the highlighted parameter in univariate analysis as a candidate variable for multivariate analyses, which were significantly correlated with AcomA aneurysm formation.

Non-adjusted and adjusted models are shown in Table 3. In the crude model, WSS correlated with AcomA aneurysm formation (HR = 1.39, 95% CI: 1.20 to 1.60, $p < 0.0001$). In the minimally adjusted model (adjusted age, gender), the effect size also had a significant correlation (HR = 1.43, 95% CI: 1.23 to 1.67, $p < 0.0001$). After adjusting other covariates, we still identified the significance in the fully adjusted model (HR = 1.87, 95% CI: 1.36 to 2.56, $p < 0.0001$). For the purpose of the sensitivity analysis, we also handled WSS as a categorical variable (quartile), and the same trend was observed as well (*p* for trend was 0.0009).

The results of the two-piecewise linear regression model

WSS ranging between 7.8 and 12.3 dyne/cm^2 showed a significant correlation between WSS and the formation of AcomA aneurysms (HR 2.0, 95% CI: 1.3-2.8, $p < 0.001$). The risk of AcomA aneurysm formation increased one-fold for each additional unit of WSS (Table 4, Fig. 2).

Discussion

Our study showed that the WSS ($p < 0.0001$), the angle between the A1 and A2 segments of the ACA ($p < 0.001$), hypertension (grade II) ($p = 0.007$), FBG (> 6.0 mmol/L) ($p = 0.005$), and dominant A1 ($p < 0.001$) were significant parameters in the formation of AcomA aneurysms. We found that the magnitude of the WSS ranged between 7.8 and 12.3 dyne/cm^2 and had a significant association with AcomA aneurysm formation (HR 2.0, 95% CI: 1.3-2.8, $p < 0.001$), consistent with the two-piecewise linear regression model. The probability of AcomA aneurysm formation increased one-fold for each additional unit of WSS.

An accurate criterion is essential for implementation of the diagnosis and therapeutic challenges in the management of intracranial aneurysms. Among the criteria of clinic and

Table 1 Baseline characteristics of participants

WSS (quartile)	Q1	Q2	Q3	Q4	*p* value	*p* value*
Case	47	51	48	53		
AcomA aneurysm					< 0.001	-
No	30 (63.83%)	41 (80.39%)	28 (58.33%)	19 (35.85%)		
Yes	17 (36.17%)	10 (19.61%)	20 (41.67%)	34 (64.15%)		
CWT	3.62 ± 0.87	3.39 ± 0.96	3.88 ± 1.12	3.48 ± 1.11	0.100	0.077
Age	57.70 ± 10.26	60.12 ± 11.02	60.38 ± 8.39	55.51 ± 12.74	0.078	0.191
Different age grades					0.200	-
< 40	3 (6.38%)	4 (7.84%)	0 (0.00%)	8 (15.09%)		
40-60	21 (44.68%)	22 (43.14%)	24 (50.00%)	23 (43.40%)		
> 60	23 (48.94%)	25 (49.02%)	24 (50.00%)	22 (41.51%)		
Gender					0.780	-
Male	21 (44.68%)	27 (52.94%)	26 (54.17%)	28 (52.83%)		
Female	26 (55.32%)	24 (47.06%)	22 (45.83%)	25 (47.17%)		
Angle between A1 and A2 segments of ACA	101.95 ± 7.20	101.87 ± 7.20	103.75 ± 6.57	105.20 ± 7.50	0.057	0.107
Dominant A1					0.007	-
No	27 (57.45%)	43 (84.31%)	32 (66.67%)	29 (54.72%)		
Yes	20 (42.55%)	8 (15.69%)	16 (33.33%)	24 (45.28%)		
Hypertension					0.401	-
No	33 (70.21%)	37 (72.55%)	38 (79.17%)	32 (60.38%)		
Grade I	7 (14.89%)	6 (11.76%)	3 (6.25%)	5 (9.43%)		
Grade II	6 (12.77%)	8 (15.69%)	7 (14.58%)	15 (28.30%)		
Grade III	1 (2.13%)	0 (0.00%)	0 (0.00%)	1 (1.89%)		
Diabetes					0.845	-
No	42 (89.36%)	46 (90.20%)	41 (85.42%)	43 (81.13%)		
Diabetes with FBS ≤ 6.0 mmol/L	3 (6.38%)	3 (5.88%)	4 (8.33%)	7 (13.21%)		
Diabetes with FBS > 6.0 mmol/L	2 (4.26%)	2 (3.92%)	3 (6.25%)	3 (5.66%)		
FBG					0.191	-
Normal	39 (82.98%)	44 (86.27%)	39 (81.25%)	37 (69.81%)		
≤ 6.0 mmol/L	3 (6.38%)	1 (1.96%)	0 (0.00%)	3 (5.66%)		
> 6.0 mmol/L	5 (10.64%)	6 (11.76%)	9 (18.75%)	13 (24.53%)		
Atherosclerosis					0.796	-
No	39 (82.98%)	45 (88.24%)	39 (81.25%)	44 (83.02%)		
Yes	8 (17.02%)	6 (11.76%)	9 (18.75%)	9 (16.98%)		
Hyperlipidemia					0.347	-
No	32 (68.09%)	42 (82.35%)	33 (68.75%)	39 (73.58%)		
Yes	15 (31.91%)	9 (17.65%)	15 (31.25%)	14 (26.42%)		
CAD					0.031	-
No	44 (93.62%)	38 (74.51%)	43 (89.58%)	47 (88.68%)		
Yes	3 (6.38%)	13 (25.49%)	5 (10.42%)	6 (11.32%)		
Smoking					0.405	-
No	41 (87.23%)	41 (80.39%)	38 (79.17%)	39 (73.58%)		
Yes	6 (12.77%)	10 (19.61%)	10 (20.83%)	14 (26.42%)		
Drinking					0.360	-
No	40 (85.11%)	39 (76.47%)	34 (70.83%)	43 (81.13%)		
Yes	7 (14.89%)	12 (23.53%)	14 (29.17%)	10 (18.87%)		

Statistical results are reported as mean ± SD or number (%).

*Continuous variable was obtained by Kruskal-Wallis rank sum test. If the count variable had a theoretical number <10, the probability was calculated accurately using Fisher's exact test

Table 2 The results of univariate analysis

Variables	Mean±SD/*N* (%)	AcomA aneurysm	
		OR and 95% CI	*p* value
WSS	8.6 ± 2.3	1.39 (1.20, 1.60)	< 0.0001
CWT	3.6 ± 1.0	1.2 (0.9, 1.5)	0.277
Age	58.4 + 10.9	1.0 (1.0, 1.0)	0.116
Different age grades			
< 40	15 (7.5%)	1.0	
40-60	90 (45.2%)	0.4 (0.1, 1.2)	0.101
> 60	94 (47.2%)	1.4 (0.5, 4.0)	0.585
Gender			
Male	102 (51.3%)	1.0	
Female	97 (48.7%)	1.5 (0.8, 2.6)	0.193
Angle between A1 and A2 segments of ACA	103.2 ± 7.2	1.1 (1.1, 1.2)	< 0.001
Dominant A1			
No	131 (65.8%)	1.0	
Yes	68 (34.2%)	32.5 (14.1, 75.1)	< 0.001
Hypertension			
No	140 (70.4%)	1.0	
Grade I	21 (10.6%)	1.1 (0.4, 2.9)	0.832
Grade II	36 (18.1%)	2.8 (1.3, 6.0)	0.007
Grade III	2 (1.0%)	1.8 (0.1, 29.4)	0.680
Diabetes			
No	172 (86.4%)	1.0	
Diabetes with FBS ≤ 6.0 mmol/L	17 (8.5%)	1.0 (0.4, 2.8)	0.969
Diabetes with FBS > 6.0 mmol/L	10 (5.0%)	1.0 (0.3, 3.6)	0.965
FBG			
Normal	159 (79.9%)	1.0	
≤ 6.0 mmol/L	7 (3.5%)	Inf. (0.0, Inf)	0.985
> 6.0 mmol/L	33 (16.6%)	3.0 (1.4, 6.5)	0.005
Atherosclerosis			
No	167 (83.9%)	1.0	
Yes	32 (16.1%)	1.2 (0.5, 2.5)	0.702
Hyperlipidemia			
No	146 (73.4%)	1.0	
Yes	53 (26.6%)	1.2 (0.6, 2.2)	0.641
CAD			
No	172 (86.4%)	1.0	
Yes	27 (13.6%)	0.4 (0.1, 1.0)	0.041
Smoking			
No	159 (79.9%)	1.0	
Yes	40 (20.1%)	0.8 (0.4, 1.7)	0.645
Drinking			
No	156 (78.4%)	1.0	
Yes	43 (21.6%)	1.2 (0.6, 2.4)	0.708

geometric morphology, local hemodynamics are the main predictors of intracranial aneurysm formation and rupture. Increasing publications involving CFD are in favor of a high WSS with intracranial aneurysm growth and low WSS producing rupture [4, 5, 8–10, 18, 19], albeit a growing number of such proposals are still controversial. Other researchers have presented different views with opposite results [20–22]. Shojima et al [21] suggested that in contrast to the pathogenic

Table 3 The results of multivariable analysis

Exposure	Crude model (HR, 95% CI, *p*)	Minimally adjusted model (HR, 95% CI, *p*)	Fully adjusted model (HR, 95% CI, *p*)
WSS	1.39 (1.20, 1.60) < 0.0001	1.43 (1.23, 1.67) < 0.0001	1.87 (1.36, 2.56) 0.0001
WSS (quartile)			
Q1	1.0	1.0	1.0
Q2	0.43 (0.17, 1.07) 0.0701	0.40 (0.16, 1.01) 0.0523	3.60 (0.45, 28.86) 0.2273
Q3	1.26 (0.55, 2.88) 0.5831	1.20 (0.52, 2.81) 0.6670	11.89 (1.61, 87.79) 0.0152
Q4	3.16 (1.39, 7.16) 0.0059	3.69 (1.58, 8.65) 0.0026	23.53 (3.09, 179.37) 0.0023
p for trend	0.0005	0.0002	0.0009

Non-adjusted model adjusted for: None

Adjust I model adjusted for: gender; age

Adjust II model adjusted for: CWT; age; different age grades; gender; angle between A1 and A2 segments of ACA; dominant A1; hypertension; diabetes; FBG; atherosclerosis; hyperlipidemia; CAD; smoking; drinking

effect of a high WSS in the initiating phase, a low WSS may facilitate aneurysm growth. We partially approved these points. Herein we propose that this controversy is probably related to the absence of accepted standards for the threshold of high or low WSS. What thresholds of high or low WSS separately vary in aneurysm development remains unclear and thus may result in divergent and controversial findings. It is also important to note that some studies have calculated the magnitude of WSS in ruptured and unruptured aneurysms [3, 5, 23]; however, the magnitude of WSS reported varies, and the threshold of high or low WSS has rarely been reported. In addition, multivariable analysis is usually taken into consideration for controversial high versus low WSS parameters [9, 10, 24]. Few researchers have studied the threshold effect of the WSS on AcomA aneurysm formation further using the two-piecewise linear regression model. We identified the threshold of WSS in the parent artery affecting AcomA aneurysm formation using a two-piecewise linear regression model ranging from 7.8 to 12.3 dyne/cm^2, which is partially inconsistent with high or low WSS theory, as suggested by Meng [4] and Can et al [8]. Notably, some studies have reported that WSS values in the range of 4-15 dyn/cm^2 are considered normal on the basis of endothelial cells [6]. Malek et al [6] demonstrated that arterial-level shear stress (> 15 dyne/cm^2) induces endothelial quiescence and an atheroprotective gene expression profile, while low shear stress (< 4 dyne/cm^2) stimulates an atherogenic phenotype; however, this normal range of WSS distinguishes the atherosclerosis-related endothelial function and phenotype rather than intracranial aneurysm-related vascular remodeling. Regardless of the differences in WSS values, the result is application using different techniques to measure flow at different locations in the arterial network [25, 26]. It also has been reported that the normal mean WSS levels range from 9.5 to 15.0 dyn/cm^2 in the common carotid artery using high-resolution echo Doppler or ultrasound share rate estimation [25, 27, 28]. Gnasso et al [27] reported the mean WSS as 12.1 ± 3.1 dyn/cm^2, and Samijo et al [28] reported the mean WSS as 12.4 ± 2.0 dyn/cm^2 in normal populations. The findings of Gnasso et al [27] and Samijo et al [28] agreed with our criterion derived from the threshold effect of the WSS in the parent artery using two-piecewise linear regression models, suggesting that WSS ranged between 7.8 and 12.3 dyne/cm^2, and independently characterized the AcomA aneurysm formation.

Table 4 The results of the two-piecewise linear regression model

Inflection point of WSS(per 0.1 change)	Effect size (HR)	95% CI	*p* value
≤ 7.8	0.7	0.5 to 1.1	0.116
7.8-12.3	2.0	1.3 to 2.8	< 0.001
> 12.3	8.7	0.7 to 109	0.093

Adjust II model adjusted for: CWT; age; different age grades; gender; angle between A1 and A2 segments of ACA; dominant A1; hypertension; diabetes; FBG; atherosclerosis; hyperlipidemia; CAD; smoking; drinking

WSS can be evaluated noninvasively and reliably using an ultrasound-based technique, which is a common approach in vivo [13–15, 29, 30]. As a widely used alternative to direct measurement of near-wall velocities, Doppler studies estimate WSS from an assumed velocity profile, which has been assumed to exhibit a parabolic (i.e., Poiseuille) profile. It has been demonstrated that a Poiseuille parabolic model of velocity distribution across the arterial lumen provides a useful estimate of WSS [31]; however, some researchers have proposed that the departure from an ideal Poiseuille may lead to errors in calculating WSS [32]. At present, few studies have demonstrated the deviation involved in estimating WSS via the Poiseuille law. The Sui et al study [31], based on MRA, reported that the Poiseuille approach led to a slightly (~10%) higher WSS value compared with a 3D paraboloid-fitting method because of the neglect of diameter variations during the cardiac cycle. A more thorough study conducted by Mynard et al [32] detailed how the assumptions would affect the results,

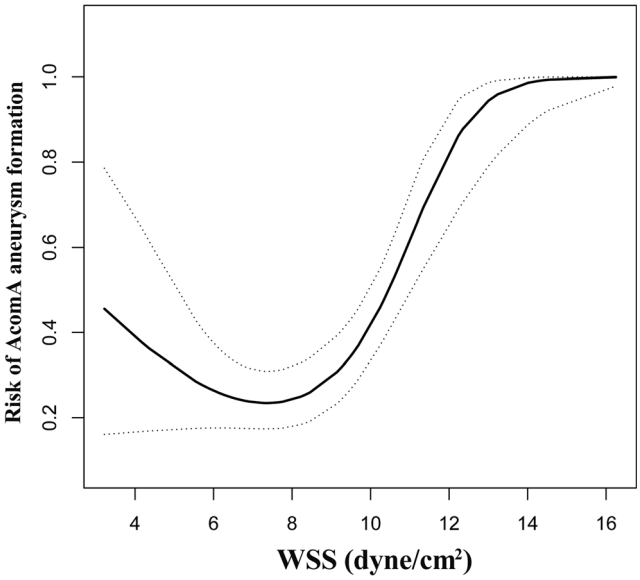

Fig. 2 The illustrated curved line relation between WSS and AcomA aneurysm formation. The area between two dotted lines is expressed as a 95% CI. Each point shows the magnitude of the WSS and is connected to form a continuous line. The magnitude of the WSS is not correlated with AcomA aneurysm formation when it is ≤ 7.8 dyne/cm^2 or > 12.3 dyne/cm^2. Conversely, the magnitude of the WSS ranged between 7.8 and 12.3 dyne/cm^2 and showed a significant correlation with the formation of AcomA aneurysms. The risk of AcomA aneurysm formation increases as the WSS increases

including cylindrical geometry, steady flow, and Newtonian flow. They analyzed errors in the estimation of WSS by the maximum Doppler velocity and pointed out an important consequence of velocity profile skewing; specifically, WSS is likely to vary circumferentially around the vessel wall, being higher near regions of high velocity. In vivo blood flow is pulsatile and non-Newtonian. Because the vessel is not a cylindrical structure and the vessel walls are not rigid, even a relatively axisymmetric and nearly fully developed profile could be associated with substantial circumferential variation in WSS, probably resulting in deviations. Mynard et al [32] also found that there was no significant difference in percent variations between axisymmetric (type I), skewed (type II), and crescent (type III) cases. Nevertheless, cycle-averaged WSS varies circumferentially by ± 60% about the circumferential mean. Because these assumptions in the Poiseuille law are not generally met in the arterial circulation, the estimation of WSS using these expressions is only approximate. Even though it was different from the WSS measured with the CFD technique, the result is still an objective indicator of the WSS in the ACA.

Furthermore, it has been proposed that the disturbing variables, like blood viscosity, velocity, arterial inner diameter, hematocrit, and atherosclerosis, may be associated with the WSS values [6, 27, 33–38]. Physiologically, WSS reflects a hemodynamic force that resides within the vascular endothelial surface [3, 6]. WSS is a direct product of complicated hemodynamic blood flow. Box et al [36] have documented that a decrease in flow and an increase in inner diameter result in a corresponding decrease in WSS, whereas a decrease in blood viscosity will reduce WSS [6, 27]. Other researchers have focused on the correlation between the presence of atherosclerosis and the WSS and found that atherosclerotic plaque deposition accelerates the arterial wall remodeling during progression of atherosclerosis, causing arteries to harden and narrow and increasing the tortuosity of the vasculature [6]. Atherosclerosis is prone to result in a smaller arterial inner diameter, thus forcing an increase in blood flow velocity in the elderly. Therefore, it is reasonable to find that a high WSS calculated according to Poiseuille's law would increase. Box et al [37] propose a whole-blood viscosity modeling in which the viscosity is dependent on the hematocrit. They also demonstrated that flow and arterial inner diameter changes have a significant influence on WSS values, which is the same for blood viscosity, but to a lesser extent. Nevertheless, WSS depends more heavily on hematocrit when low plasma viscosity exists. This is also supported by previous studies in which the relationship between blood viscosity and hematocrit is well approximated by an exponential function [38].

In our study, WSS was calculated according to the Poiseuille law and equation. Although the Poiseuille law and the resulting Hagen Poiseuille formula are based on specific assumptions regarding blood flow, it is still an appealing and fascinating method due to its simplicity and is utilized by several techniques in clinical practice. One of the advantages of our method described before is that the input data used to calculate WSS (Vm and ID) are being routinely recorded and reproduced during ultrasonography. It should be noted that this model provides a useful estimation of WSS and has been confirmed in a growing number of new studies [13–15, 29, 30]. It is a simple and accessible method and can be widely applied in primary care facilities and community hospitals in many developing countries because of the relatively low resource intensity.

Because the WSS of the parent artery is closely related to aneurysm formation, it is very important for predicting aneurysm formation with the assistance of screening and monitoring WSS. If the threshold of the WSS associated with a high risk of aneurysm formation is established, patients who have the WSS of the parent artery in this particular range can be monitored judiciously. Early intervention is of utmost importance in such situations to curtail adverse consequences.

Our study had some limitations. First, blood flow in vivo is pulsatile, non-Newtonian, and not in a cylindrical structure, the walls of which are not rigid. The major drawback of this approach is the assumption of a linear velocity distribution and the fact that only the central peak velocity is used to measure the WSS. Thus, hemodynamic parameters calculated by the Poiseuille law according to the formula are just an approximate value. Second, procedural-related factors may

also affect the accuracy of the results. Third, we only measured the WSS of the parent artery rather than that in the AcomA aneurysm itself. The direct WSS in the AcomA aneurysm could not be detected using our clinical method.

Conclusions

WSS ranged between 7.8 and 12.3 dyne/cm^2 and was found to be one of the reliable hemodynamic parameters in the formation of AcomA aneurysms. The probability of AcomA aneurysm formation increases one-fold for each additional unit of WSS. An ultrasound-based TCCD technique is a simple and accessible noninvasive method for detecting WSS in vivo and thus can be applied as a screening tool for evaluating the probability of aneurysm formation in primary care facilities and community hospitals because of the relatively low resource intensity.

Acknowledgements We acknowledge further polishing of the article to improve the language and the rationality of the content provided by Dr. Tamrakar Karuna (CMS-Teaching Hospital, Bharatpur, Chitwan, Nepal) and the helpful comments on this article received from the reviewers. We also appreciate Prof. Chi Chen (Department of Health Statistics of Guizhou University of TCM, Guiyang City, China) for his important contribution to the professional statistical analysis in the study.

Funding This study received funding from the Science and Technology Project Foundation of Guangdong Province (grant no. 2016A020215098), Key Project of Clinical Research of Southern Medical University (grant no. LC2016ZD024), and National Key Research Development Program (grant no. 2016YFC1300804, 2016YFC1300800).

Compliance with ethical standards

Guarantor The scientific guarantor of this publication is Chuan-Zhi Duan who works in the Department of Neurosurgery, Zhujiang Hospital, Southern Medical University.

Conflict of interest The authors of this manuscript declare no relationships with any companies, whose products or services may be related to the subject matter of the article.

Statistics and biometry Prof. Chi Chen, who has significant statistical expertise (Department of Health Statistics of Guizhou University of TCM, Guiyang City, China), kindly provided statistical advice for this manuscript.

Informed consent This is a retrospective and cross-sectional study. The data are anonymous, and the requirement for written informed consent was waived by the Institutional Review Board. However, the informed consent concerning the DSA procedure was signed by each patient before the operation.

Ethical approval Approval for this study was obtained from the local Institutional Review Board of the participating centers. Ethics approval was obtained from the Institutional Review Board of Southern Medical University Zhujiang Hospital and the First Affiliated Hospital of Zhengzhou University.

Methodology
- retrospective
- cross-sectional study
- multicenter study

References

1. Horiuchi T, Tanaka Y, Hongo K (2005) Surgical treatment for aneurysmal subarachnoid hemorrhage in the 8th and 9th decades of life. Neurosurgery 56:469–475 discussion 469-475
2. Leipzig TJ, Morgan J, Horner TG, Payner T, Redelman K, Johnson CS (2005) Analysis of intraoperative rupture in the surgical treatment of 1694 saccular aneurysms. Neurosurgery 56:455–468 discussion 455-468
3. Qiu T, Jin G, Xing H, Lu H (2017) Association between hemodynamics, morphology, and rupture risk of intracranial aneurysms: a computational fluid modeling study. Neurol Sci 38:1009–1018
4. Meng H, Tutino VM, Xiang J, Siddiqui A (2014) High WSS or low WSS? Complex interactions of hemodynamics with intracranial aneurysm initiation, growth, and rupture: toward a unifying hypothesis. AJNR Am J Neuroradiol 35:1254–1262
5. Karmonik C, Yen C, Grossman RG, Klucznik R, Benndorf G (2009) Intra-aneurysmal flow patterns and wall shear stresses calculated with computational flow dynamics in an anterior communicating artery aneurysm depend on knowledge of patient-specific inflow rates. Acta Neurochir (Wien) 151:479–485 discussion 485
6. Malek AM, Alper SL, Izumo S (1999) Hemodynamic shear stress and its role in atherosclerosis. JAMA 282:2035–2042
7. Meng H, Wang Z, Hoi Y et al (2007) Complex hemodynamics at the apex of an arterial bifurcation induces vascular remodeling resembling cerebral aneurysm initiation. Stroke 38:1924–1931
8. Can A, Du R (2016) Association of hemodynamic factors with intracranial aneurysm formation and rupture: systematic review and meta-analysis. Neurosurgery 78:510–520
9. Skodvin TØ, Evju Ø, Helland CA, Isaksen JG (2017) Rupture prediction of intracranial aneurysms: a nationwide matched case-control study of hemodynamics at the time of diagnosis. J Neurosurg:1–7
10. Fukazawa K, Ishida F, Umeda Y et al (2015) Using computational fluid dynamics analysis to characterize local hemodynamic features of middle cerebral artery aneurysm rupture points. World Neurosurg 83:80–86
11. Kaspera W, Ładziński P, Larysz P et al (2014) Morphological, hemodynamic, and clinical independent risk factors for anterior communicating artery aneurysms. Stroke 45:2906–2911
12. Ye J, Zheng P, Hassan M, Jiang S, Zheng J (2017) Relationship of the angle between the A1 and A2 segments of the anterior cerebral artery with formation and rupture of anterior communicating artery aneurysm. J Neurol Sci 375:170–174
13. Krejza J, Mariak Z, Walecki J, Szydlik P, Lewko J, Ustymowicz A (1999) Transcranial color Doppler sonography of basal cerebral arteries in 182 healthy subjects: age and sex variability and normal reference values for blood flow parameters. AJR Am J Roentgenol 172:213–218
14. Irace C, Carallo C, De Franceschi MS et al (2012) Human common carotid wall shear stress as a function of age and gender: a 12-year follow-up study. Age (Dordr) 34:1553–1562
15. Stolz E, Kaps M, Kern A, Dorndorf W (1999) Frontal bone windows for transcranial color-coded duplex sonography. Stroke 30:814–820
16. Velcheva I, Antonova N, Damianov P, Dimitrov N (2010) Common carotid artery hemodynamic factors in patients with cerebral infarctions. Clin Hemorheol Microcirc 45:233–238

17. Carallo C, Irace C, Pujia A et al (1999) Evaluation of common carotid hemodynamic forces. Relations with wall thickening. Hypertension 34:217–221
18. Longo M, Granata F, Racchiusa S et al (2017) Role of hemodynamic forces in unruptured intracranial aneurysms: an overview of a complex scenario. World Neurosurg 105:632–642
19. Kawaguchi T, Nishimura S, Kanamori M et al (2012) Distinctive flow pattern of wall shear stress and oscillatory shear index: similarity and dissimilarity in ruptured and unruptured cerebral aneurysm blebs. J Neurosurg 117:774–780
20. Liu J, Xiang J, Zhang Y et al (2014) Morphologic and hemodynamic analysis of paraclinoid aneurysms: ruptured versus unruptured. J Neurointerv Surg 6:658–663
21. Shojima M, Oshima M, Takagi K et al (2004) Magnitude and role of wall shear stress on cerebral aneurysm: computational fluid dynamic study of 20 middle cerebral artery aneurysms. Stroke 35: 2500–2505
22. Sugiyama S, Meng H, Funamoto K et al (2012) Hemodynamic analysis of growing intracranial aneurysms arising from a posterior inferior cerebellar artery. World Neurosurg 78:462–468
23. Chien A, Tateshima S, Sayre J, Castro M, Cebral J, Viñuela F (2009) Patient-specific hemodynamic analysis of small internal carotid artery-ophthalmic artery aneurysms. Surg Neurol 72:444–450 discussion 450
24. Frösen J (2016) Flow dynamics of aneurysm growth and rupture: challenges for the development of computational flow dynamics as a diagnostic tool to detect rupture-prone aneurysms. Acta Neurochir Suppl 123:89–95
25. Cheng C, Helderman F, Tempel D et al (2007) Large variations in absolute wall shear stress levels within one species and between species. Atherosclerosis 195:225–235
26. Galizia MS, Barker A, Liao Y et al (2014) Wall morphology, blood flow and wall shear stress: MR findings in patients with peripheral artery disease. Eur Radiol 24:850–856
27. Gnasso A, Carallo C, Irace C et al (1996) Association between intima-media thickness and wall shear stress in common carotid arteries in healthy male subjects. Circulation 94:3257–3262
28. Samijo SK, Barkhuysen R, Willigers JM et al (2002) Wall shear stress assessment in the common carotid artery of end-stage renal failure patients. Nephron 92:557–563
29. Katritsis D, Kaiktsis L, Chaniotis A, Pantos J, Efstathopoulos EP, Marmarelis V (2007) Wall shear stress: theoretical considerations and methods of measurement. Prog Cardiovasc Dis 49:307–329
30. Liu Z, Zhao Y, Wang X et al (2016) Low carotid artery wall shear stress is independently associated with brain white-matter hyperintensities and cognitive impairment in older patients. Atherosclerosis 247:78–86
31. Sui B, Gao P, Lin Y, Gao B, Liu L, An J (2008) Assessment of wall shear stress in the common carotid artery of healthy subjects using 3.0-tesla magnetic resonance. Acta Radiol 49:442–449
32. Mynard JP, Wasserman BA, Steinman DA (2013) Errors in the estimation of wall shear stress by maximum Doppler velocity. Atherosclerosis 227:259–266
33. Nixon AM, Gunel M, Sumpio BE (2010) The critical role of hemodynamics in the development of cerebral vascular disease. J Neurosurg 112:1240–1253
34. Shakur SF, Alaraj A, Mendoza-Elias N, Osama M, Charbel FT (2018) Hemodynamic characteristics associated with cerebral aneurysm formation in patients with carotid occlusion. J Neurosurg :1-6
35. Jing L, Zhong J, Liu J et al (2016) Hemodynamic effect of flow diverter and coils in treatment of large and giant intracranial aneurysms. World Neurosurg 89:199–207
36. Box FM, van der Grond J, de Craen AJ et al (2007) Pravastatin decreases wall shear stress and blood velocity in the internal carotid artery without affecting flow volume: results from the PROSPER MRI study. Stroke 38:1374–1376
37. Box FM, van der Geest RJ, Rutten MC, Reiber JH (2005) The influence of flow, vessel diameter, and non-Newtonian blood viscosity on the wall shear stress in a carotid bifurcation model for unsteady flow. Invest Radiol 40:277–294
38. Dormandy JA (1974) Medical and engineering problems of blood viscosity. Biomed Eng 9:284–289